

THE CRYSTAL STRUCTURE OF MORINITE

F. C. HAWTHORNE

Department of Earth Sciences, University of Manitoba, Winnipeg, Manitoba R3T 2N2

ABSTRACT

The crystal structure of morinite, $\text{Ca}_2\text{Na}[\text{Al}_2\text{F}_4(\text{OH})(\text{H}_2\text{O})_2(\text{PO}_4)_2]$, a 9.454(3), b 10.692(4), c 5.444(2) Å, β 105.46(2)°, V 530.38 Å³, $Z=2$, space group $P2_1/m$, has been solved by Patterson and Fourier methods and refined by a full-matrix least-squares method to an R index of 2.8% for 1095 observed (3σ) reflections. Equivalent $\text{Ca}(\text{H}_2\text{O})\text{F}_3\text{O}_4$ polyhedra are fused by face-sharing across the mirror plane, and these doublets are repeated by the 2_1 operation to form a staggered edge-sharing chain parallel to the b axis. Chain linkage occurs through an NaF_2O_3 trigonal bipyramid and an $[\text{Al}_2\text{F}_4(\text{OH})(\text{H}_2\text{O})_2(\text{PO}_4)_2]$ polyhedral cluster. This cluster contains a dimer of corner-sharing octahedra $[\text{Al}_2\text{F}_4(\text{OH})(\text{H}_2\text{O})_2\text{O}_4]$ further linked by two (PO_4) tetrahedra. This is the first reported occurrence of an unpolymerized cluster. $[\text{M}_2\phi_7\text{XO}_4]_2$, where M is an octahedrally coordinated cation, X a tetrahedrally coordinated cation, and ϕ an unspecified anion. The structures of several complex transition metal phosphates are based on the polymerization of a topologically identical cluster, whose persistence in low-temperature secondary phosphates suggests that it, or a major fragment of it, is an important complex in low-temperature aqueous pegmatitic fluids.

SOMMAIRE

La structure de la morinite $\text{Ca}_2\text{Na}[\text{Al}_2\text{F}_4(\text{OH})(\text{H}_2\text{O})_2(\text{PO}_4)_2]$ est établie dans $P2_1/m$, par la méthode Patterson et les séries de Fourier, pour la maille a 9.454(3), b 10.692(4), c 5.444(2) Å, β 105.46(2)°, avec $Z = 2$. L'affinement par moindres carrés, à matrice complète, laisse un résidu $R = 0.028$ pour 1095 réflexions observées (3σ). Deux polyèdres $\text{Ca}(\text{H}_2\text{O})\text{F}_3\text{O}_4$ sont équivalents par réflexion dans un miroir contenant une face qui leur est commune; l'axe 2_1 les répète en quinconce avec arête partagée, le long d'une chaîne parallèle à $b[010]$. La liaison intercatène est assurée par une dipyramide trigonale NaF_2O_3 et un groupement polyédrique $[\text{Al}_2\text{F}_4(\text{OH})(\text{H}_2\text{O})_2(\text{PO}_4)_2]$. Ce dernier est constitué par un dimère $[\text{Al}_2\text{F}_4(\text{OH})(\text{H}_2\text{O})_2\text{O}_4]$ comprenant deux octaèdres unis par un sommet et reliés en plus par deux tétraèdres PO_4 . C'est la première fois qu'on rencontre un groupe $[\text{M}_2\phi_7(\text{XO}_4)_2]$ qui ne soit pas polymérisé; ici, M occupe une position octaédrique, X une position tétraédrique, et ϕ représente un groupement anionique quelconque.

Plusieurs phosphates des métaux de transition ont leur structure fondée sur la polymérisation d'un groupe topologiquement identique, dont la persistance parmi les phosphates secondaires de basse température est un signe de son importance dans les fluides pegmatitiques aqueux.

(Traduit par la Rédaction)

INTRODUCTION

Morinite, a rare hydrothermal hydrous fluoro-phosphate, is found in association with montebasite, apatite, augelite and wardite in pegmatitic environments. The few available chemical analyses are summarized by Fisher & Runner (1958) and Fisher (1960), who proposed the chemical formula $\text{Ca}_2\text{Na}_2\text{Al}_4(\text{PO}_4)_4(\text{OH}_x\text{F}_{5-x})_2(5-x)\text{H}_2\text{O}$, with $x \sim 1\frac{1}{2}$. From precession and Weissenberg photographs, Fisher & Runner (1958) determined the unit cell and showed the space group to be $P2_1$ or $P2_1/m$; in addition, crystal morphology suggested that it was centric. However, Fisher (1960) indicated that preliminary results of a structural analysis of morinite showed it to be non-centric.

The current study was prompted by the recent work on the structure of whitlockite (Gopal & Calvo 1972, Gopal *et al.* 1974, Kostiner & Rea 1976) and on its relation to the structures of apatite and the large-cation arsenates, phosphates, vanadates and sulfates (Gopal & Calvo 1971, 1973; Dickens *et al.* 1973, Moore 1973, 1976). Extensive heating experiments on morinite (Fisher 1960) showed that it transforms to the apatite structure at $\sim 400^\circ\text{C}$ and to the whitlockite structure at $\sim 800^\circ\text{C}$. Knowledge of the morinite structure hopefully will aid in the interpretation of these transformations.

EXPERIMENTAL

Single-crystal X-ray precession photographs exhibit monoclinic symmetry with systematic absences $0k0$, $k=2n+1$, consistent with space groups $P2_1/m$ and $P2_1$. Cell dimensions were determined by least-squares refinement of 15 reflections automatically aligned on a 4-circle

diffractometer. The values obtained, a 9.454(3), b 10.692(4), c 5.444(2) Å, β 105.46(2)°, agree closely with those obtained by Fisher & Runner (1958).

An equidimensional fragment of ~ 0.10 mm diameter was used to collect the intensity data according to the experimental method of Hawthorne & Grundy (1976). Two standard reflections were monitored every 50 reflections; no significant change in their intensities was observed during the data collection. A total of 1252 reflections was measured over one asymmetric unit to a maximum 2θ of 60° ($\sin\theta/\lambda = 0.704$). The data were corrected for Lorentz, polarization and background effects and reduced to structure factors. No absorption corrections were performed as preliminary calculations showed them to be negligible for this crystal ($\mu = 16.8 \text{ cm}^{-1}$). A reflection was considered as observed if its magnitude exceeded that of three standard deviations based on counting statistics. Of the 1252 unique reflections, 1095 were classed as observed.

STRUCTURE SOLUTION AND REFINEMENT

Scattering curves for neutral atoms were taken from Cromer & Mann (1968), with anomalous dispersion coefficients from Cromer & Liberman (1970). R indices are of the form given in Table 1 and are expressed as percentages.

The three-dimensional Patterson synthesis, $P(uvw)$, showed that most atoms are situated at $y = \pm 1/4$. A solution was found for two atoms in general positions, initially assigned as Ca and P. Elimination of Ca–Ca, P–P and Ca–P vectors allowed the location of two more atoms situated on the mirror plane at $y = 1/4$; the vector intensities now indicated that P

TABLE 1. MISCELLANEOUS INFORMATION

a	9.454(3) Å	Crystal size	~ 0.10 mm
b	10.692(4)	Rad/Mono	Mo/C
c	5.444(2)	Total No. of $ F_o $	1252
β	105.46(2)°	No. of $ F_o > 3\sigma$	1095
V	530.4(1)	Final R (obs. data)	2.8%
Space Group	$P2_1/m$	Final R_w (obs. data)	3.2%
Unit cell contents	$2 [Ca_2NaAl_2F_4(OH)(H_2O)_2(PO_4)_2]$		
Temperature factor form used:	$\exp \left[- \sum_{i=1}^3 \sum_{j=1}^3 h_i h_j \beta_{ij} \right]$		
$R = \frac{\sum (F_o - F_c)}{\sum F_o }$			
$R_w = \left[\frac{\sum w(F_o - F_c)^2}{\sum w F_o^2} \right]^{1/2}$, $w = 1$			

TABLE 2. ATOMIC POSITIONS AND EQUIVALENT ISOTROPIC TEMPERATURE FACTORS FOR MORINITE

	x	y	z	$B_{\text{equiv.}} (\text{Å}^2)$
Ca	0.14521(7)	0.58288(6)	0.2400(1)	0.65(1)
Al	0.2576(1)	0.4062(1)	0.7733(2)	0.49(2)
Na	0.6885(2)	1/4	0.2083(4)	1.29(3)
P(1)	0.0438(1)	1/4	0.3715(2)	0.43(2)
P(2)	0.5087(1)	1/4	0.6415(2)	0.48(2)
O(1)	0.9699(3)	1/4	0.0854(6)	0.77(5)
O(2)	0.2287(3)	1/4	0.8962(6)	0.62(5)
O(3)	0.6754(3)	1/4	0.7650(6)	0.74(5)
O(4)	0.4748(4)	1/4	0.3535(6)	0.90(5)
O(5)	0.9292(3)	1/4	0.5248(6)	0.74(5)
O(6)	0.3554(2)	0.0419(2)	0.1304(4)	0.73(4)
O(7)	0.4423(2)	0.1340(2)	0.7346(4)	0.78(4)
O(8)	0.1433(2)	0.1320(2)	0.4416(4)	0.63(3)
F(1)	0.0968(2)	0.0328(2)	0.8605(3)	0.76(3)
F(2)	0.7150(2)	0.0587(2)	0.3392(3)	0.80(3)
H(1)	0.169(8)	1/4	0.985(13)	1.0*
H(2)	0.426(5)	0.992(5)	0.162(9)	1.0*
H(2)	0.382(5)	0.112(5)	0.218(9)	1.0*

*fixed during refinement

occupied the two special positions and Al occupied a general position. This model yielded an R index (Table 1) of 37%. Subsequent difference Fourier synthesis located all the remaining non-hydrogen atoms. Full-matrix least-squares refinement of all positional variables with isotropic temperature factors fixed at 1.5 Å^2 and all anions considered as oxygen converged to an R index of 11.5%. By inclusion of variable isotropic temperature factors, the refinement converged to an R index of 4.9%. The isotropic temperature factors for two anions were $\sim 0.0 \text{ Å}^2$ as compared to 0.7–1.1 Å^2

TABLE 3. ANISOTROPIC TEMPERATURE FACTORS ($\times 10^4$)

	β_{11}	β_{22}	β_{33}	β_{12}	β_{13}	β_{23}
Ca	15(1)	14(1)	75(2)	-2(1)	11(1)	-6(1)
Al	11(1)	9(1)	66(3)	1(1)	11(1)	1(1)
Na	47(2)	19(2)	132(7)	0	21(3)	0
P(1)	11(1)	9(1)	50(4)	0	9(2)	0
P(2)	9(1)	11(1)	61(4)	0	9(2)	0
O(1)	21(4)	17(3)	64(11)	0	-1(5)	0
O(2)	17(3)	11(3)	81(11)	0	22(5)	0
O(3)	8(3)	15(3)	114(12)	0	7(5)	0
O(4)	28(4)	19(3)	87(11)	0	15(5)	0
O(5)	15(3)	20(3)	84(11)	0	23(5)	0
O(6)	16(2)	16(2)	84(7)	5(2)	8(2)	2(3)
O(7)	15(2)	14(2)	119(8)	1(2)	22(3)	5(3)
O(8)	19(2)	11(2)	66(7)	2(2)	7(3)	1(3)
F(1)	14(2)	19(2)	91(6)	-5(1)	15(3)	3(3)
F(2)	25(2)	11(2)	97(6)	3(1)	11(3)	-1(3)

TABLE 4. INTERATOMIC DISTANCES (Å) AND ANGLES (°) IN

MORINITE			
P(1)-O(1)	1.528(3)	Ca-O(1)	2.545(2)
P(1)-O(5)	1.534(3)	Ca-O(3)	2.486(2)
P(1)-O(8) x2	1.558(2)	Ca-O(5)	2.408(2)
<P(1)-O>	1.545	Ca-O(6)	2.591(2)
		Ca-O(8)	2.545(2)
P(2)-O(3)	1.541(3)	Ca-F(1)	2.272(2)
P(2)-O(4)	1.514(3)	Ca-F(1)'	2.344(2)
P(2)-O(7) x2	1.539(2)	Ca-F(2)	2.334(2)
<P(2)-O>	1.533	<Ca-O,F>	2.438
A1-O(2)	1.844(2)	Na-O(3)	2.383(4)
A1-O(6)	1.996(2)	Na-O(4)	2.359(4)
A1-O(7)	1.862(2)	Na-O(5)	2.463(4)
A1-O(8)	1.886(2)	Na-F(2) x2	2.156(2)
A1-F(1)	1.830(2)	<Na-O,F>	2.303
A1-F(2)	1.782(2)		
<A1-O,F>	1.867		

O(1)-O(5)	2.972(5)	O(1)-Ca-O(5)	73.7(1)
O(5)-O(3)	3.025(4)	O(5)-Ca-O(3)	76.7(1)
O(3)-F(2)	3.185(3)	O(3)-Ca-F(2)	83.1(1)
F(2)-O(6)	3.309(3)	F(2)-Ca-O(6)	84.2(1)
O(6)-O(8)	3.103(3)	O(6)-Ca-O(8)	74.3(1)
O(8)-F(1)	3.252(3)	O(8)-Ca-F(1)	83.3(1)
F(1)-F(1)'	2.762(3)	F(1)-Ca-F(1)'	73.5(1)
F(1)'-O(1)	3.016(3)	F(1)'-Ca-O(1)	77.3(1)
<O,F-O,F>	3.078	<O,F-Ca-O,F>	78.3

Hydrogen bonds

O(2)-H(1)	0.84(7)		
H(1)-O(1)	2.10(7)	O(2)-H(1)-O(1)	161(7)
O(2)-O(1)	2.898(5)		
O(6)-H(2)	0.83(5)		
O(6)-H(3)	0.89(5)		
H(3)-H(2)	1.40(7)	H(2)-O(6)-H(3)	109(4)
H(2)-O(7)	1.82(5)	O(6)-H(2)-O(7)	124(2)
H(3)-O(4)	1.77(5)	O(6)-H(3)-O(4)	165(4)
O(6)-O(7)	2.641(3)		
O(6)-O(4)	2.638(3)		

P(1) tetrahedron

O(1)-O(5)	2.521(4)	O(1)-P(1)-O(5)	110.9(2)
O(1)-O(8) x2	2.519(3)	O(1)-P(1)-O(8) x2	109.4(1)
O(5)-O(8) x2	2.526(3)	O(5)-P(1)-O(8) x2	109.6(1)
O(8)-O(8)	2.520(5)	O(8)-P(1)-O(8)	107.9(2)
<O-O>	2.522	<O-P(1)-O>	109.5

P(2) tetrahedron

O(3)-O(4)	2.521(5)	O(3)-P(2)-O(4)	111.2(1)
O(3)-O(7) x2	2.498(3)	O(3)-P(2)-O(7) x2	108.4(1)
O(4)-O(7) x2	2.512(4)	O(4)-P(2)-O(7) x2	110.8(1)
O(7)-O(7)	2.477(5)	O(7)-P(2)-O(7)	107.2(2)
<O-O>	2.503	<O-P(2)-O>	109.5

A1 octahedron

O(2)-O(6)	2.681(3)	O(2)-A1-O(6)	88.4(1)
O(2)-O(7)	2.704(4)	O(2)-A1-O(7)	93.7(1)
O(2)-O(8)	2.702(4)	O(2)-A1-O(8)	92.8(1)
O(2)-F(1)	2.616(2)	O(2)-A1-F(1)	90.8(1)
O(6)-O(7)	2.680(3)	O(6)-A1-O(7)	87.9(1)
O(6)-F(1)	2.499(3)	O(6)-A1-F(1)	81.4(1)
O(6)-F(2)	2.688(3)	O(6)-A1-F(2)	90.5(1)
O(7)-O(8)	2.858(3)	O(7)-A1-O(8)	99.4(1)
O(7)-F(2)	2.508(3)	O(7)-A1-F(2)	87.0(1)
O(8)-F(1)	2.654(3)	O(8)-A1-F(1)	91.2(1)
O(8)-F(2)	2.552(3)	O(8)-A1-F(2)	88.1(1)
F(1)-F(2)	2.517(3)	F(1)-A1-F(2)	88.4(1)
<O,F-O,F>	2.638	<O,F-A1-O,F>	90.0

Na trigonal bipyramid

O(3)-O(4)	4.135(4)	O(3)-Na-O(4)	121.4(1)
O(3)-O(5)	4.193(3)	O(3)-Na-O(5)	119.8(1)
O(4)-O(5)	4.151(3)	O(4)-Na-O(5)	118.8(1)
<O-O>	4.160	<O-Na-O>	120.0
O(3)-F(2) x2	3.668(3)	O(3)-Na-F(2) x2	107.7(1)
O(4)-F(2) x2	3.072(3)	O(4)-Na-F(2) x2	85.7(1)
O(5)-F(2) x2	2.866(3)	O(5)-Na-F(2) x2	76.4(1)
<O-F>	3.202	<O-Na-F>	89.9
		F(2)-Na-F(2)'	142.7(1)

Ca square antiprism

O(5)-F(2)	2.866(3)	O(5)-Ca-F(2)	74.3(1)
F(2)-O(8)	2.552(3)	F(2)-Ca-O(8)	62.9(1)
O(8)-F(1)	2.995(3)	O(8)-Ca-F(1)	76.7(1)
F(1)-O(5)	3.112(3)	F(1)-Ca-O(5)	83.3(1)
O(1)-F(1)'	3.114(2)	O(1)-Ca-F(1)'	79.0(1)
F(1)-O(6)	2.499(3)	F(1)'-Ca-O(6)	60.6(1)
O(6)-O(3)	3.195(3)	O(6)-Ca-O(3)	78.3(1)
O(3)-O(1)	2.867(4)	O(3)-Ca-O(1)	69.8(1)
<O-F-O,F>	2.900	<O,F-Ca-O,F>	73.1

TABLE 5. VIBRATION ELLIPSOIDS

	R.M.S. Displacement	Angle to a-axis	Angle to b-axis	Angle to c-axis
Ca	0.076(2) Å	18(7) ^o	73(6) ^o	97(4) ^o
	0.088(2)	72(7)	146(5)	121(4)
	0.106(1)	89(2)	118(3)	32(3)
Al	0.063(3)	26(13)	116(13)	105(4)
	0.073(3)	116(13)	154(13)	79(6)
	0.096(2)	87(4)	87(5)	19(4)
Na	0.104(5)	90	90	90
	0.136(4)	87(33)	90	167(33)
	0.141(4)	3(33)	90	103(33)
P(1)	0.066(4)	7(8)	90	112(8)
	0.071(4)	90	0	90
	0.084(3)	83(8)	90	22(8)
P(2)	0.060(4)	0(2)	90	105(5)
	0.078(3)	90	0	90
	0.092(3)	90(5)	90	15(5)
O(1)	0.083(9)	53(12)	90	52(12)
	0.098(8)	90	0	90
	0.112(7)	143(12)	90	37(12)
O(2)	0.068(11)	20(9)	90	125(9)
	0.081(9)	90	0	90
	0.110(7)	70(9)	90	35(9)
O(3)	0.057(12)	11(5)	90	94(5)
	0.093(8)	90	0	90
	0.128(6)	101(5)	90	4(5)
O(4)	0.104(8)	90	0	90
	0.106(7)	155(71)	90	49(71)
	0.111(7)	65(71)	90	41(71)
O(5)	0.061(12)	18(8)	90	124(8)
	0.108(8)	90	0	90
	0.112(7)	72(5)	90	34(5)
O(6)	0.072(7)	34(9)	121(9)	91(7)
	0.102(6)	120(12)	149(9)	89(30)
	0.110(5)	104(16)	90(27)	1(16)
O(7)	0.070(7)	6(10)	87(16)	111(4)
	0.089(6)	86(16)	171(7)	83(8)
	0.130(4)	85(4)	81(6)	22(4)
O(8)	0.077(7)	119(16)	30(18)	90(14)
	0.092(6)	134(32)	118(19)	110(39)
	0.098(5)	122(33)	99(23)	20(39)
F(1)	0.064(6)	22(5)	68(5)	108(4)
	0.107(4)	110(6)	39(20)	115(23)
	0.115(4)	99(9)	59(22)	31(2)
F(2)	0.077(6)	107(8)	17(8)	85(5)
	0.104(4)	153(11)	106(8)	96(12)
	0.118(4)	110(12)	96(6)	8(10)

for the remaining anions. A bond-strength calculation was carried out at this stage, using

the bond-strength curves of Brown & Wu (1976). The bond-strength sums around the two anions with zero temperature factors were ~ 1.3 v.u. (Table 6); recalculation of the bond-strength sums around these anions using bond-strength curves for cation-F bonds (I.D. Brown, pers. comm.) yielded values close to 1.0 v.u. Both the low isotropic temperature factors and the bond-strength results indicated that these anions were F rather than OH; the scattering curves were appropriately modified and refinement of all variables for an isotropic thermal model converged to an R index of 4.0%. The isotropic temperature factors of the F anions were now comparable with the remaining anions. Temperature factors were converted to anisotropic motions of the form given in Table 1, and two cycles of least-squares refinement reduced the R index to 3.2%. Inspection of a difference-Fourier map calculated at this stage revealed three significant peaks; the first was $\sim 1\text{\AA}$ from O(2) and the other two were $\sim 1\text{\AA}$ from O(6). As the preliminary bond-strength calculations indicated that O(2) was a hydroxyl anion and O(6) was a water molecule, these peaks were assumed to be due to hydrogen atoms. Insertion of three hydrogen atoms into the refinement and full-

matrix least-squares refinement of all variables (with the exception of the hydrogen-atom isotropic temperature factors which were fixed at 1.0\AA^2) resulted in convergence at R indices of 2.8 (observed reflections) and 3.4% (all data) and R_w indices of 3.2 (observed reflections) and 3.6% (all data). Observed and calculated structure factors may be obtained from The Depository of Unpublished Data, CISTI, National Research Council of Canada, Ottawa, Ontario K1A 0S2. Final atomic positions and equivalent isotropic temperature factors are presented Table 2, and anisotropic temperature-factor coefficients are listed in Table 3. Interatomic distances and angles and the magnitudes and orientations of the principal axes of the thermal ellipsoids, calculated with the program ERRORS (L. W. Finger, pers. comm.), are presented in Tables 4 and 5.

DISCUSSION

Description of the structure

Calcium is surrounded by five oxygen and three fluorine anions in a distorted square antiprismatic arrangement. This polyhedron is

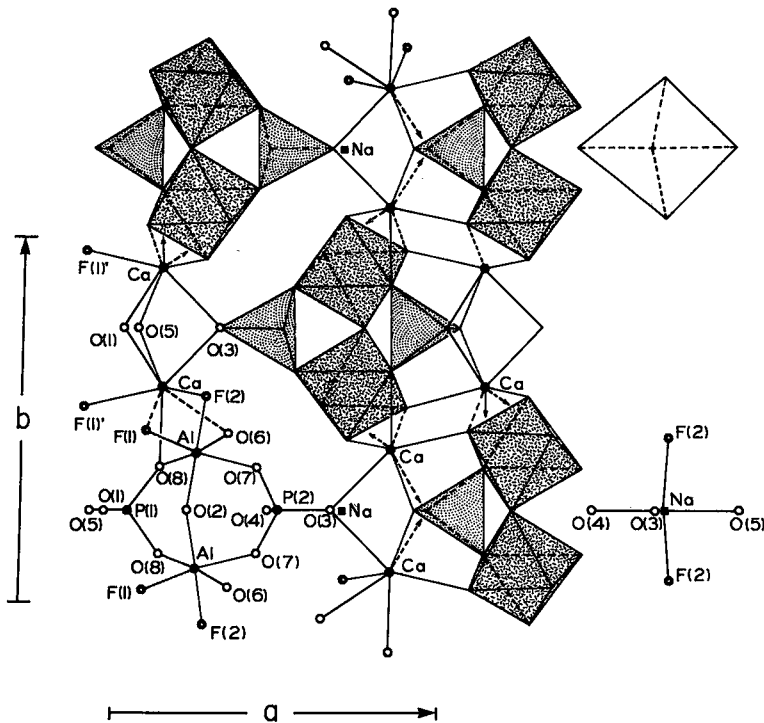


FIG. 1. The structure of morinitite projected down c^* .

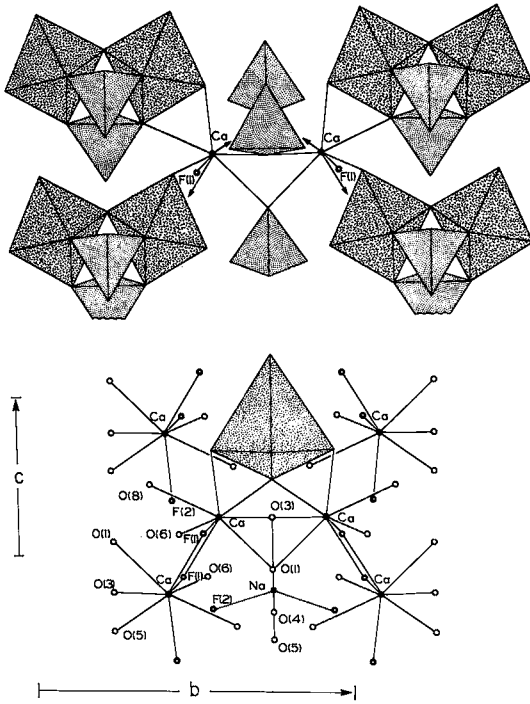


FIG. 2. The structure of morinite projected down a^* .

structure shown in Figure 1. Aluminum is surrounded by two oxygens, two fluorines, one hydroxyl and one water in a distorted octahedral arrangement. This octahedron is fused by the mirror operation to an equivalent octahedron to form a corner-sharing octahedral dimer of composition $[Al_2F_4(OH)(H_2O)_2O_4]^{7-}$. Additional linkage between the two octahedra is provided by two (PO_4) tetrahedra, resulting in a polyhedral cluster of composition $[Al_2F_4(OH)(H_2O)_2(PO_4)_2]^{5-}$ (Fig. 2). These clusters, together with the $(NaO_3F_2)^{7-}$ trigonal bipyramids, knit the staggered $[Ca_2O_5F_4(H_2O)_2]^{10-}$ chains into a continuous three-dimensional linkage.

Examination of the empirical bond-strength table for morinite (Table 6), calculated using the bond-strength curves of Brown & Wu (1976) and I. D. Brown (pers. comm.), shows that the individual bond-length variations in each of the cation coordination polyhedra correlate well with the bond-strength requirements of the coordinating anions. This table is also of particular interest with regard to the identification of fluorine anions in the structure. As indicated above, the fluorine anions were identified during refinement by their scattering power, and this identification is confirmed by bond-strength arguments. Using cation-F bond-strength curves, the bond-strength sums around both anions and cations are close to their ideal values; using cation-O bond-strength curves, the corresponding values are significantly too large.

TABLE 6. EMPIRICAL BOND STRENGTH TABLE FOR MORINITE*

	Ca	Al	Na	P(1)	P(2)	Σ^{**}	H(1)	H(2)	H(3)	Σ
O(1)	0.212 $\times 2^2$			1.292		1.716	[0.26] \ddagger			[1.980]
O(2)		0.577 $\times 2^2$				1.154	[0.78]			[1.950]
O(3)	0.250 $\times 2^2$		0.192		1.246	1.938				1.938
O(4)			0.201		1.344	1.545			[0.25] $\times 2^2$	[2.045]
O(5)	0.285 $\times 2^2$		0.167	1.270		2.007				2.007
O(6)	0.192	0.411				0.603	[0.74]	[0.71]		[2.053]
O(7)		0.553			1.253 $\times 2^2$	1.806	[0.24]			[2.046]
O(8)	0.212	0.524		1.189 $\times 2^2$		1.925				1.925
	0.274					1.070				1.070
F(1) †	0.330	0.466								
	(0.330)	(0.596)				(1.317)				(1.317)
	(0.391)									
F(2)	0.281	0.523	0.231 $\times 2^2$			1.035				1.035
	(0.338)	(0.668)	(0.295) $\times 2^2$			(1.301)				(1.301)
Σ	2.036	3.054	1.022	4.940	5.096		[1.04]	[0.98]	[0.96]	
	(2.210)	(3.329)	(1.150)							

* calculated from the bond strength curves of Brown & Wu (1976) and I.D. Brown (pers. comm.).
 ** Bond strength sum around the anions excluding hydrogen bond contributions. *** Bond strength around the anions including hydrogen bond contributions. † Values in parentheses are calculated using cation-oxygen bond strength curves for bonds involving those anions designated as fluorine.
 \ddagger Hydrogen bond strengths in square brackets are estimated so as to let the bond strength sums around both anions and cations approach their ideal values.

From the bond-strength table, O(2) and O(6) are immediately recognized as (OH) and (H₂O) groups respectively, thus confirming the H atom locations derived from difference maps in the final stages of refinement. The refined hydrogen atom positions will be significantly in error due to the effect of electron delocalization along the O–H bond. Nevertheless, a sensible pattern of hydrogen bonding is suggested by the local geometry (Fig. 3), leading to an adequate distribution of bond strengths; O(2) is a hydroxyl, a hydrogen-bond donor with O(1) as the acceptor anion. The O(2)–O(1) distance of 2.90 Å and O(2)–H(1)–O(1) angle of ~160° are typical values for an asymmetric hydrogen bond. Anion O(6) is a water molecule, a hydrogen-bond donor with O(4) and O(7) as acceptor anions. The local geometry is compatible with the range of values found by neutron diffraction in many hydrates (Baur 1972). The distribution of hydrogen-bond-strengths resulting from these arrangements leads to an adequate total bond-strength distribution in the morinite structure (Table 6).

Chemical composition

Table 7 shows a comparison of the chemical analysis for morinite from Hugo mine, Black Hills, S. Dakota (Fisher 1960) with the ideal composition for a formula unit of Ca₂NaAl₂F₄(OH)(H₂O)₂(PO₄)₂. The oxide weight percentages are very close, suggesting that the cation content does not deviate significantly from the ideal formula used in the

TABLE 7. CHEMICAL ANALYSIS OF MORINITE FROM BLACK HILLS, SOUTH DAKOTA, AND IDEAL COMPOSITION

	Fisher (1960)	Ca ₂ NaAl ₂ F ₄ (OH)(H ₂ O) ₂ (PO ₄) ₂
CaO	23.60	23.56
Na ₂ O	6.62	6.51
Al ₂ O ₃	22.33	21.41
P ₂ O ₅	30.04	29.82
F	13.31	15.96
H ₂ O	9.98	9.46
	105.88	106.72
-O=F	5.60	6.72
	100.28	100.00

structure refinement. However, the F is significantly less in the analysis of Fisher (1960) than in the ideal formula unit, and this raises the question of possible substitution of (OH) for F in the morinite structure. Recalculation of the Fisher analysis on the basis of 22 oxygens gives the cell content Ca_{3.94}Al_{4.10}P_{3.96}O₁₆[F_{6.56}(OH)_{0.37}](OH)₂(H₂O)₄; this leaves a deficiency of 1.07(F,OH) in the formula. Fisher (1960) gives a duplicate analysis for F and H₂O in the Black Hills morinite, the relevant values being 14.30% F and 10.04% H₂O; using these values in the analysis of Table 7 gives Ca_{3.94}Na_{2.00}Al_{4.10}P_{3.96}O₁₆[F_{7.05}(OH)_{0.43}](OH)₂(H₂O)₄, still leaving a deficiency of 0.52(F,OH). In the present structure refinement, the equivalent isotropic temperature factors of all the anions are extremely well-behaved, negating the possibility of any significant anion vacancies occurring in this structure. In addition, the bond-strength sums around the F(1) and F(2) positions in the structure are close to their ideal values when calculated with cation–F bond-strength curves and deviate greatly when calculated with cation–O bond-strength curves. This suggests that the extent of OH-for-F substitution in the F(1) and F(2) positions of this crystal is small, and that the chemical composition adheres closely to the ideal Ca₂NaAl₂F₄(OH)(H₂O)₂(PO₄)₂.

The morinite → apatite transformation

Extensive heating experiments by Fisher (1960) have shown that morinite transforms to an apatite-like phase at ~400°C. The apatite structure is characterized by columns of face-sharing CaO₉ polyhedra that bear little resemblance to the [Ca₂O₃F₄(H₂O)₂]¹⁰⁻ chains in morinite. This, together with the presence of the [Al₂F₄(OH)(H₂O)₂(PO₄)₂]⁵⁻ cluster in morinite, indicates that the morinite → apatite transformation is almost entirely a reconstructive phase-change.

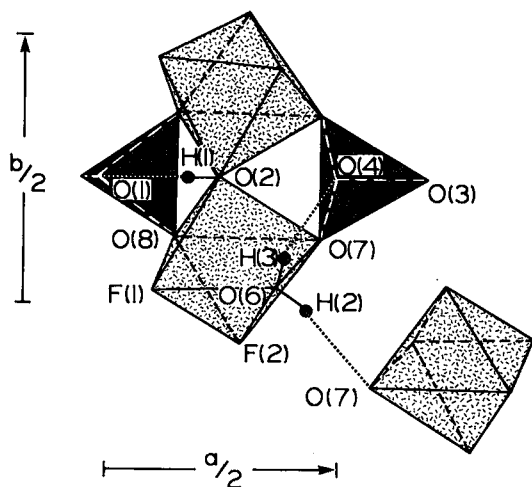


FIG. 3. Hydrogen bonding in morinite.

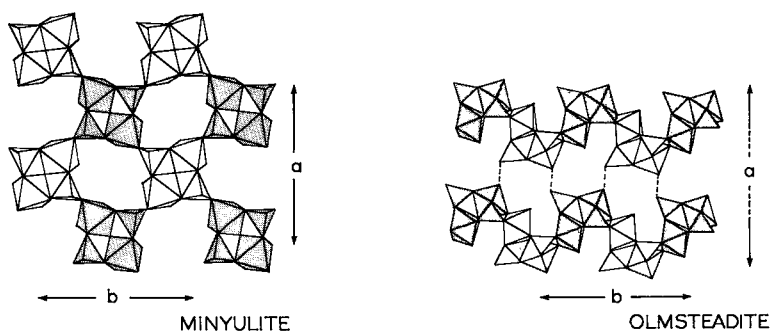


FIG. 4. Polyhedral representations of the structures of minyulite and olmsteadite; alternate $[M_2\phi_7(XO_4)_2]$ clusters are shaded. The spiral chains in olmsteadite have been separated along x for clarity.

The $[M_2\phi_7(XO_4)_2]$ cluster

The $[Al_2F_4(OH)(H_2O)_2(PO_4)_2]^{5-}$ cluster in morinite is the first reported occurrence of an unpolymerized $[M_2\phi_7(XO_4)_2]$ cluster in a phosphate structure; here, according to the usage of Moore (1970), M and X correspond to cations at octahedral and tetrahedral centres, respectively, and ϕ indicates an unspecified anion at a polyhedral vertex. A topologically equivalent cluster $[Fe^{3+}_2(OH)(H_2O)_4O_2(SO_4)_2]^{3-}$ occurs in the structure of copiapite (Fanfani *et al.* 1973), but these are linked into chains by bridging non-cluster (SO_4) tetrahedra; as the bond strengths involved in the inter-cluster linkage are as strong as the intra-cluster linkages, the clusters cannot be considered isolated, as is the case in morinite. Several complex phosphate structures are based on a polymerization of $[M_2\phi_7(XO_4)_2]$ clusters topologically identical to the cluster found in morinite.

Simple repeated corner-sharing of octahedra in a *trans* arrangement results in an $[M\phi_5]^\infty$ octahedral chain of the form $[M_2\phi_6(XO_4)_2]$ that corresponds to arrangements II and III of Moore (1970). Corner-sharing between octahedra and tetrahedra of adjacent $[Al_2F(H_2O)_2O_2(PO_4)_2]$ clusters forms the basis of the structure of minyulite (Kampf 1977), as illustrated in Figure 4a. The resulting open sheets provide eight-fold coordination for K, and adjacent sheets are linked by hydrogen bonding. A more complex corner-sharing linkage is observed in olmsteadite, $K_2Fe^{2+}_2[Fe^{2+}_2(Nb,Ta)^{5+}_2(H_2O)_4O_4(PO_4)_4]$, whose structure was reported by Moore *et al.* (1976). As shown in Figure 4b, adjacent $[Fe^{2+}(Nb,Ta)O_6(H_2O)(PO_4)_2]$ clusters link by sharing octahedral vertices to form an $[M\phi_5]^\infty$ chain. This differs from the $[M\phi_5]^\infty$ chain described earlier in

that the octahedral vertices linking the clusters together are in a *cis* arrangement, with the octahedral vertex linking the two octahedra within a single cluster. Additional linkage between clusters is provided by the sharing of octahedral-tetrahedral vertices; one tetrahedral vertex in each cluster is shared with an octahedral vertex (*trans* with respect to the intra-cluster linking vertex) of the adjacent cluster. Thus the structure of olmsteadite can be considered as spiral chains of condensed $[M_2\phi_7(XO_4)_2]$ clusters that are cross-linked by shared tetrahedral-octahedral vertices, $Fe^{2+}O_6$ octahedra and KO_8 cubes.

Several structures of considerable complexity are based on polymerization of $[M_2\phi_7(XO_4)_2]$ clusters by inter-cluster octahedral edge-sharing. Perhaps one of the simpler structures that can be constructed in this manner is hureaulite, $Mn^{2+}_3(H_2O)_4[PO_3(OH)]_2[PO_4]_2$, studied by Moore & Araki (1973). Adjacent $[Mn^{2+}_2(H_2O)_3O_4[PO_3(OH)](PO_4)]$ clusters link by sharing octahedral edges; one vertex of the shared edge is also a vertex of a $PO_3(OH)$ tetrahedron whereas the other vertex is *trans* to the intra-cluster octahedral vertex linkage. The resulting element is a kinked chain of composition $[Mn^{2+}_2(H_2O)_3O_2[PO_3(OH)](PO_4)]$ that runs parallel to the b axis (Fig. 5a). These chains are cross-linked in the a direction by sharing an octahedral edge and a tetrahedral vertex with an $Mn^{2+}O_6$ octahedron that is similarly linked to the next adjacent chain. A similar but distinct linkage is found in the structures of phosphoferrite, $Fe^{2+}_3(H_2O)_3(PO_4)_2$, and kryzhanovskite, $Fe^{2+}_3(OH)_3(PO_4)_2$, the structures of which are reported by Moore (1971) and Moore & Araki (1976). For phosphoferrite, adjacent $[Fe^{2+}_2(H_2O)_3O_4(PO_4)_2]$ clusters link by sharing octahedral edges to form a kinked chain

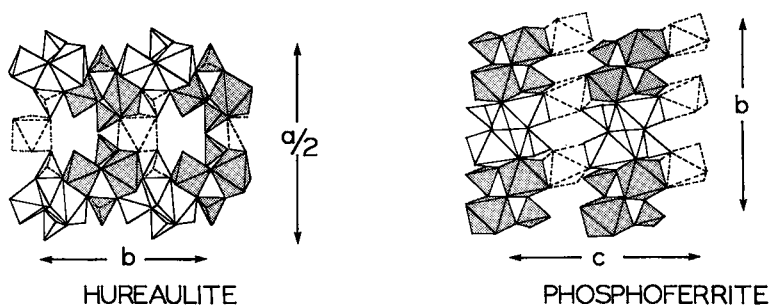


FIG. 5. Polyhedral representations of the structures of hureaulite and phosphoferrite; alternate $[M_2O_7(XO_4)_2]$ clusters are shaded. Linking octahedra are shown by broken lines.

of composition $[Fe^{2+}_2(H_2O)_3O_2(PO_4)_2]$. This differs from the corresponding chain in hureaulite in that both vertices of the shared octahedral edge are in a *cis* relationship with the intra-cluster linkage vertex. Adjacent chains share edges with linking $Fe^{2+}(H_2O)_2O_4$ octahedra to give a sheet-like aspect to the structure (Fig. 5).

Melonjosephite, $Ca_2[(Fe^{2+}Fe^{3+})_2(OH)_2(PO_4)_4]$, whose structure was solved by Kampf & Moore (1977), can be constructed from $[M_2O_7(XO_4)_2]$ clusters. Adjacent $[Fe^{2+}_{0.5}Fe^{3+}_{0.5}]_2(OH)_2O_5(PO_4)_2$ clusters share an octahedral edge to form a chain. There are two distinct edge-sharing configurations: the edge shared between Fe(2) octahedra consists of *cis* and *trans* octahedral vertices (with respect to the intra-cluster vertex linkage) and does not involve a cluster tetrahedral vertex; the edge shared between Fe(1) octahedra is a *cis-trans* edge involving a cluster vertex. Figure 6a shows an exploded view of the melonjosephite structure that emphasizes these staggered chain

elements. As is apparent from Figure 6, these chains condense by octahedral edge-sharing and tetrahedral-octahedral vertex-sharing to form rather open sheets parallel to $\{010\}$. The remaining tetrahedral vertices knit two adjacent sheets to complete the linkage. Whitmoreite, $Fe^{2+}Fe^{3+}_2(OH)_2(H_2O)_4(PO_4)_2$, whose structure is described by Moore *et al.* (1974), is based on octahedral edge-sharing between adjacent $[Fe^{3+}_2(OH)_3O_4(PO_4)_2]$ clusters. As with phosphoferrite, both vertices involved in the shared octahedral edge are *cis* with respect to the intra-cluster vertex linkage; however, both shared vertices also coincide with a cluster tetrahedral vertex. The resulting staggered chain links to adjacent chains by vertex sharing between adjacent octahedra, and adjacent octahedra and tetrahedra, as shown in the exploded view of the whitmoreite structure in Figure 6b. This produces an open sheet that is linked to adjacent sheets above and below by $Fe^{3+}(H_2O)_2O_4$ octahedra.

Thus, several apparently diverse minerals

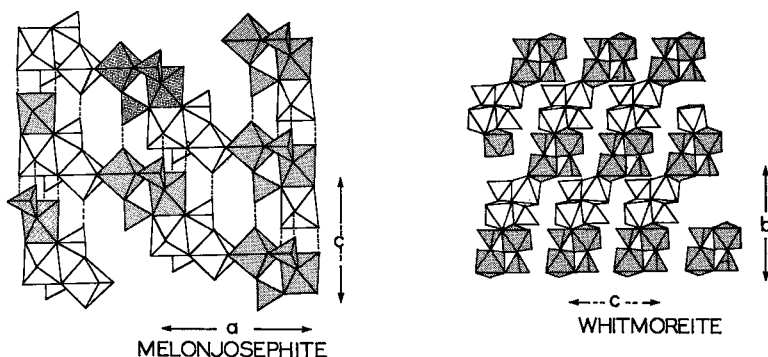


FIG. 6. Exploded polyhedral representations of the structures of melonjosephite and whitmoreite; alternate $[M_2O_7(XO_4)_2]$ clusters are shaded.

seem to have structures based on polymerization of the $[M_2\phi_7(XO_4)_2]$ cluster. It is notable that all the structures discussed here are low-temperature secondary phosphates that have crystallized from an aqueous fluid in a pegmatitic environment. The presence of this $[M_2\phi_7(XO_4)_2]$ cluster in these diverse structures suggests that the same cluster, or at least a major fragment of it, is present in the fluid phase. Kampf (1977) has remarked on the stability of octahedral fluoride complexes of aluminum in aqueous solutions, and has suggested that the $[Al_2O_{11}]$ octahedral dimer will form only when the bridging ligand is F^- . This may be so under the synthesis conditions of minyulite, but the existence of the OH-bridged $[Al_2F_4(OH)(H_2O)_2O_4]$ dimer in the structure of morinite indicates that this is not generally the case; the morinite dimer is more fluorine-rich than the minyulite dimer and yet is still hydroxyl-bridged, suggesting that the hydroxyl-bridged $[Al_2O_{11}]$ dimer is more stable than the fluorine-bridged dimer under the conditions of formation of morinite. Certainly, the persistence of the $[M_2\phi_7(XO_4)_2]$ cluster in several diverse low-temperature phosphate structures for $M = Fe^{2+}, Fe^{3+}, Mn, Al, Nb^{5+}$ suggests that this cluster is a very stable entity and may occur as a complex in the low-temperature pegmatitic fluids from which these minerals crystallize.

ACKNOWLEDGEMENTS

The author is indebted to the late Dr. C. Calvo, Materials Research Institute, McMaster University, Hamilton, Ontario, for suggesting this study; the Institute is also thanked for their cooperation in the collection of the intensity data. The patronage of the National Research Council of Canada (grants to Professors R. B. Ferguson and A. C. Turnock) and the University of Manitoba are gratefully acknowledged.

REFERENCES

- BAUR, W. H. (1972): Prediction of hydrogen bonds and hydrogen atom positions in crystalline solids. *Acta Cryst.* B28, 1456-1465.
- BROWN, I. D. & WU, K. K. (1976): Empirical parameters for calculating cation-oxygen bond valences. *Acta Cryst.* B32, 1957-1959.
- CROMER, D. T. & LIBERMAN, D. (1970): Relativistic calculation of anomalous scattering factors for X-rays. *J. Chem. Phys.* 53, 1891-1898.
- & MANN, J. B. (1968): X-ray scattering factors computed from numerical Hartree-Fock wave functions. *Acta Cryst.* A24, 321-324.
- DICKENS, B., BROWN, W. E. KRUGER, G. J. & STEWART, J. M. (1973): $Ca_4(PO_4)_2O$, tetracalcium diphosphate monoxide. Crystal structure and relationships to $Ca_5(PO_4)_3OH$ and $K_3Na(SO_4)_2$. *Acta Cryst.* B29, 2046-2056.
- FANFANI, L., NUNZI, A., ZANAZZI, P. F. & ZANZARI, A. R. (1973): The copiapite problem: the crystal structure of a ferrian copiapite. *Amer. Mineral.* 58, 314-322.
- FISHER, D. J. (1960): Morinite-apatite-whitlockite. *Amer. Mineral.* 45, 645-667.
- & MCCONNELL, D. (1969): Aluminum-rich apatite. *Science* 164, 551-553.
- & RUNNER, J. J. (1958): Morinite from the Black Hills. *Amer. Mineral.* 43, 585-594.
- GOPAL, R. & CALVO, C. (1971): Crystal structure of $Ca_3(AsO_4)_2$. *Can. J. Chem.* 49, 1036-1046.
- & —— (1972): Structural relationship of whitlockite and $\beta Ca_3(PO_4)_2$. *Nature Phys. Sci.* 237, 30-32.
- & —— (1973): The structure of $Ca_3(VO_4)_2$. *Z. Krist.* 137, 67-85.
- & ——, ITO, J. & SABINE, W. K. (1974): Crystal structure of synthetic Mg-whitlockite, $Ca_{18}Mg_2H_2(PO_4)_{14}$. *Can. J. Chem.* 52, 1152-1164.
- HAWTHORNE, F. C. & GRUNDY, H. D. (1976): The crystal chemistry of the amphiboles. IV. X-ray and neutron refinements of the crystal structure of tremolite. *Can. Mineral.* 14, 334-345.
- KAMPF, A. R. (1977): Minyulite: its atomic arrangement. *Amer. Mineral.* 62, 256-262.
- & MOORE, P. B. (1977): Melonjosephite, calcium iron hydroxy phosphate: its crystal structure. *Amer. Mineral.* 62, 60-66.
- KOSTINER, E. & REA, J. R. (1976): The crystal structure of manganese-whitlockite, $Ca_{18}Mn_2H_2(PO_4)_{14}$. *Acta Cryst.* B32, 250-253.
- MOORE, P. B. (1970): Structural hierarchies among minerals containing octahedrally coordinating oxygen. I. Stereoisomerism among corner-sharing octahedral and tetrahedral chains. *Neues Jahrb. Mineral. Monatsh.*, 163-173.
- (1971): The $Fe^{2+}_3(H_2O)_n(PO_4)_2$ homologous series: crystal-chemical relationships and oxidized equivalents. *Amer. Mineral.* 56, 1-17.
- (1973): Bracelets and pinwheels: a topological-geometrical approach to the calcium orthosilicate and alkali sulphate structures. *Amer. Mineral.* 58, 32-42.

- (1976): The glaserite, $K_3Na[SO_4]_2$, structure type as a "super" dense-packed oxide: evidence for icosahedral geometry and cation-anion mixed layer packings. *Neues Jahrb. Mineral. Abh.* 127, 187-196.
- & ARAKI, T. (1973): Hureaulite, $Mn^{2+}_5(H_2O)_4[PO_3(OH)]_2[PO_4]_2$: its atomic arrangement. *Amer. Mineral.* 58, 302-307.
- & —— (1976): A mixed-valence solid-solution series: crystal structures of phosphoferrite, $Fe^{II}_3(H_2O)_3[PO_4]_2$, and kryzhanovskite, $Fe^{III}_3(OH)_3[PO_4]_2$. *Inorg. Chem.* 15, 316-321.
- , ——, KAMPF, A. R. & STEELE, I. M. (1976): Olmsteadite, $K_2Fe^{2+}_2[Fe^{3+}_2(Nb,Ta)^{5+}_2O_4(H_2O)_4(PO_4)_4]$, a new species, its crystal structure and relation to vauxite and montgomeryite. *Amer. Mineral.* 61, 5-11.
- , KAMPF, A. R. & IRVING, A. J. (1974): Whitmoreite, $Fe^{2+}Fe^{3+}_2(OH)_2(H_2O)_4[PO_4]_2$, a new species: its description and atomic arrangement. *Amer. Mineral.* 59, 900-905.

Received May 1978; revised manuscript accepted September 1978.